Voltage-gated potassium currents in stratum oriens–alveus inhibitory neurones of the rat CA1 hippocampus

Lei Zhang and Chris J. McBain *

Unit on Cellular and Synaptic Physiology, Laboratory of Cellular and Molecular Neurophysiology, NICHD-NIH, 9000 Rockville Pike, Bethesda MD 20892-4495, USA

1. Voltage-activated K^+ currents were recorded from visually identified inhibitory interneurones of the CA1 stratum oriens–alveus region in neonatal rat hippocampal slices using outside-out patch and whole-cell voltage clamp techniques.

2. Outward currents comprised both a transient and a sustained component when elicited from a holding potential of −90 mV. Tail current analysis of current reversal potentials showed that outward currents were carried by potassium ions.

3. The transient current, I_A, was activated with a time to peak within 5 ms, inactivated with a time constant of ~15 ms at 0 mV and possessed half-activation at −14 mV. Half-inactivation of the transient current occurred at −71 mV. At −90 mV, the transient current recovered from inactivation with a time constant of 142 ms.

4. Activation of currents from a holding potential of −50 mV permitted isolation of the sustained current, I_K. In Ca^{2+}-free conditions the sustained current showed rapid activation, reaching about 80% of its maximum within 1·5 ms, and showed little inactivation during 1 s depolarizing steps. The majority of sustained outward currents showed no voltage-dependent inactivation. In ~20% of cells, a slow time-dependent inactivation of the sustained current was observed, suggesting the presence of a second type of sustained current in these cells.

5. A Ca^{2+}-dependent K^+ current comprised a significant portion of the total sustained current; this current was activated at voltages positive to −30 mV and showed no time-dependent inactivation over a 1 s depolarizing step. This current component was removed in Ca^{2+}-free conditions or by iberiotoxin.

6. Low concentrations of 4-AP (50 μM) attenuated both the transient and sustained current components recorded in a Ca^{2+}-free solution. Higher concentrations of 4-AP (<10 mM) were without further effect on the sustained current but completely blocked the transient current with an IC_{50} of 1·8 mM. TEA blocked the sustained current with an IC_{50} of 7·9 mM without significantly reducing the transient current. Both current components were resistant to dendrotoxin (500 nM).

Voltage-dependent potassium currents of hippocampal neurones have been extensively characterized in both primary cultures and in the *in vitro* slice preparation (Zbicz & Weight, 1985; Rogawski, 1986; Numann, Wadman & Wong, 1987; Sah, Gibb & Gage, 1988; Ficker & Heinemann, 1992). The temporal overlap of a variety of divergent potassium current phenotypes determines the resting membrane potential and the threshold for action potential initiation, underlies the action potential repolarization and after-hyperpolarization (AHP), and determines the spike frequency and discharge characteristics of these neurones (for review see Halliwell, 1990).

The inhibitory interneurones of the stratum oriens–alveus (st. O–A) of the CA1 subfield are predominantly GABAergic and exert extensive and powerful inhibition onto pyramidal cells (Traub & Miles, 1991; McBain, DiChiara & Kauer, 1994). Under physiological conditions these cells provide a constant barrage of tonic inhibitory input to pyramidal cells (McBain & Dingledine, 1992), and play a crucial role in

* To whom correspondence should be addressed.

regulating the excitability of the pyramidal neurones through both feedback and feedforward inhibition of the CA1 pyramidal neurones (for review see Traub & Miles, 1991). The st. O–A cell's action potential properties are distinct from those of the pyramidal neurone. Action potentials are brief (~1 ms) and followed by a prominent, but brief, AHP (~200 ms) with no evidence for spike after-depolarization (Lacaille, Meuller, Kunkel & Schwartzkroin, 1987). In addition, spontaneous, weakly accommodating action potential firing occurs over a wide range of membrane potentials. Although much is known about the neurochemistry, their role in the local circuits and the basic electrical properties of inhibitory cells (for review see Lacaille *et al.* 1987), little is known about the kinetic or pharmacological properties of voltage gated potassium channels expressed on these cells. Likewise, limited information exists concerning the mRNA expression patterns of cloned potassium channel subunits in hippocampal interneurones. Members of the *Shaw* (Kv3.1 and Kv3.2) and *Shaker* (Kv1.4) subfamilies are preferentially expressed in subsets of hippocampal interneurones but not pyramidal cells (Weiser *et al.* 1994; Rettig *et al.* 1992). These observations suggest that hippocampal interneurones have a distinct compliment of voltage-gated potassium channels whose temporal overlap is likely to determine their characteristic action potential phenotypes.

In the present study, we have used both outside-out patch and whole-cell voltage clamp recordings to characterize the transient and sustained components of voltage-dependent outward currents from visually identified st. O–A interneurones maintained in the neonate hippocampal slice preparation. In the accompanying paper we then determined the roles of these potassium currents in action potential repolarization and the generation of the AHPs of these cells using current clamp recording techniques.

METHODS

Hippocampal slices

Hippocampal slices were prepared as described previously (McBain, 1994). Briefly Sprague–Dawley rats (11–20 days old) were killed by decapitation following deep anaesthesia using isoflurane. The brain was rapidly removed and placed in ice-cold artificial cerebrospinal fluid (ACSF) (mM): NaCl, 130; $NaHCO_3$, 24; KCl, 3·5; NaH_2PO_4, 1·25; $CaCl_2$, 1·5; $MgSO_4$, 1·5; glucose, 10; saturated with 95% O_2–5% CO_2 (pH 7·4, 307 mosmol l^{-1}). Using a Vibratome (Oxford series 1000; Polysciences, Warrington, PA, USA), 250–350 μm-thick sagittal slices were cut from the middle third of the hippocampus. Slices were allowed a recovery period of 45 min before use, during which they were held in oxygenated media at 27 °C. During recording, slices were bathed in a tissue chamber of 1 ml capacity and perfused at a rate of 2–4 ml min^{-1} with ACSF at room temperature (24–26 °C). A nominally Ca^{2+}-free, Cd^{2+}-containing (0·1 mM) ACSF was used where indicated in the text. Tetrodotoxin (TTX, 0·5–1 μM) and the α-amino-3-hydroxy-5-methyl-4-isoxazolepropionic acid (AMPA) receptor antagonist 6,7-dinitroquinoxaline-2,3-dione (DNQX; 20 μM) were added to the perfusate to block voltage-dependent Na^+ channels and excitatory synaptic activity, respectively. All drugs were applied in known concentrations by direct addition to the perfusate, via a three-way tap. Phenol Red was added to the drug solution in order to monitor its ingress and egress.

Tight seal (>1 GΩ) outside-out patch and whole-cell recordings (Hamill, Marty, Neher, Sakmann & Sigworth, 1981; Edwards, Konnerth, Sakmann & Takahashi, 1989) were obtained from the cell bodies of 117 interneurones located in st. O–A. Electrodes were fabricated from borosilicate glass and were not fire polished. Patch electrodes had resistances of 3–6 MΩ when filled with (mM): potassium gluconate, 130; NaCl, 10; $MgCl_2$, 1; Na_2ATP, 2; NaGTP, 0·3; Hepes, 10; EGTA, 0·6; buffered to pH 7·4 and 275 mosmol l^{-1}. Biocytin (0·4%) was added to the internal solution for histochemical study after recording. In several experiments glutathione (5 mM) was added and Mg^{2+} omitted from the internal solution as indicated in the text. All data are represented as means ± standard error of the mean. Seals were attained by the method originally described by Blanton, LoTurco & Kriegstein, (1989). The electrode was positioned under visual control within the st. O–A of CA1; individual cells were visualized using a Zeiss water-immersion objective modified with Hoffman optics (overall magnification, ×500). Cell sealing and breakthrough to whole-cell mode were performed under current clamp conditions to allow an initial evaluation of cell viability. The series resistance usually ranged from 12–33 MΩ; membrane potentials were not corrected for these errors. Outside-out patches were then excised from the soma after an appropriate time (>2–20 min) to permit sufficient biocytin leakage into the neurone under study. Linear leak current and the capacitive artifacts were digitally subtracted using P/4 or P/8 subtraction prior to data acquisition and analysis. All recordings were obtained with an Axopatch-1D amplifier (Axon Instruments). Records were filtered at 1–5 kHz and digitized at 3–10 kHz on an 80486-based computer. Data were analysed using the N05 (kindly provided by Dr S. Traynelis, Emory University, Atlanta, GA, USA) and the pCLAMP suite of programs (Axon Instruments). Signals were also stored unfiltered on video tape for later analysis.

Histology

Following all interneurone recordings, intact slices were fixed in 4% paraformaldehyde for at least 24 h. After immersion in phosphate buffered saline (PBS)–30% sucrose, slices were cut into 50–70 μm sections on a freezing microtome. Biocytin staining was visualized using an Avidin–horseradish peroxidase reaction (Vectastain ABC standard kit; Vector Labs, Burlingame, CA, USA), enhanced with $NiNH_4SO_4$ (1%) and $CoCl_2$ (1%). This enhancement step was essential for complete visualization of the interneurone axon. The slices were mounted and dehydrated on gelatin-coated glass slides for camera lucida reconstruction and photography. In some cases recordings were found to be made from ectopic pyramidal neurones located in st. O–A. Data obtained from these cells were discarded.

Drugs and chemicals

The following compounds were purchased from Sigma: 4-amino-pyridine (4-AP), apamin, 8-bromo cAMP, carbachol, histamine, noradrenaline, and tetraethylammonium chloride (TEA). 6,7-Dinitroquinoxaline-2,3-dione (DNQX) was obtained from Tocris Cookson. Dendrotoxin was obtained from Alomone Labs (Jerusalem, Israel). Iberiotoxin was purchased from Alomone Labs, Peptides International (Louisville, KY, USA) and Research Biochemicals International (Natick, MA, USA).

RESULTS

Morphology of st. oriens–alveus inhibitory neurones

In the present study and in the accompanying manuscript (Zhang & McBain, 1995), recordings were obtained from a total of 236 inhibitory neurones located at the border of st. O–A. Of these inhibitory neurones, eighty-five were successfully processed for biocytin staining and morphologically characterized following electrophysiological recording. All cells identified as st. O–A interneurones belonged to either of the two cell types described previously by McBain *et al.* (1994). Sixty-eight of eighty-five inhibitory neurones had morphologies which corresponded to horizontally oriented inhibitory neurones (Fig. 1*A*). The dendritic tree of this cell type typically lies parallel to the st. pyramidale and was never found to cross over the pyramidal cell layer into st. radiatum. The axons of this cell type ramify in st. radiatum and st. lacunosum–moleculare (see McBain *et al.* 1994, for details). The remaining seventeen cells possessed vertically oriented dendrites which passed across st. pyramidale into st. radiatum and had axons which ramified exclusively in the pyramidal cell layer (Fig. 1*B*). Often the dendrites of both cells possessed stubby or thorn-like spines. No differences in the action potential waveform or voltage-gated potassium current properties could be attributed to the morphology of the cells and consequently all data from both cell types were combined.

Outward currents of st. O–A interneurones

Despite the relatively small physical profile of interneurones compared with pyramidal neurones, interneurones possess an electrotonic profile which is likely to introduce space-clamp errors into voltage clamp data (Thurbon, Field & Redman, 1994). Consequently all voltage-dependent and kinetic analyses were restricted to data obtained from outside-out patches. Some pharmacological data were obtained from recordings made in whole-cell mode. Macroscopic outward currents were elicited by depolarizing steps when the internal face of the cell was dialysed with 140 mM internal K^+ and bathed in ACSF containing 3·5 mM K^+, 0 Ca^{2+} and 0·1 mM Cd^{2+}. From a holding potential of −50 mV, depolarization steps evoked only a sustained current component which showed little time-dependent inactivation. In all experiments the test pulse was delivered at a frequency of 0·1 Hz. In contrast, when depolarizing steps were delivered from a holding potential of −90 mV or alternatively were preceded by a

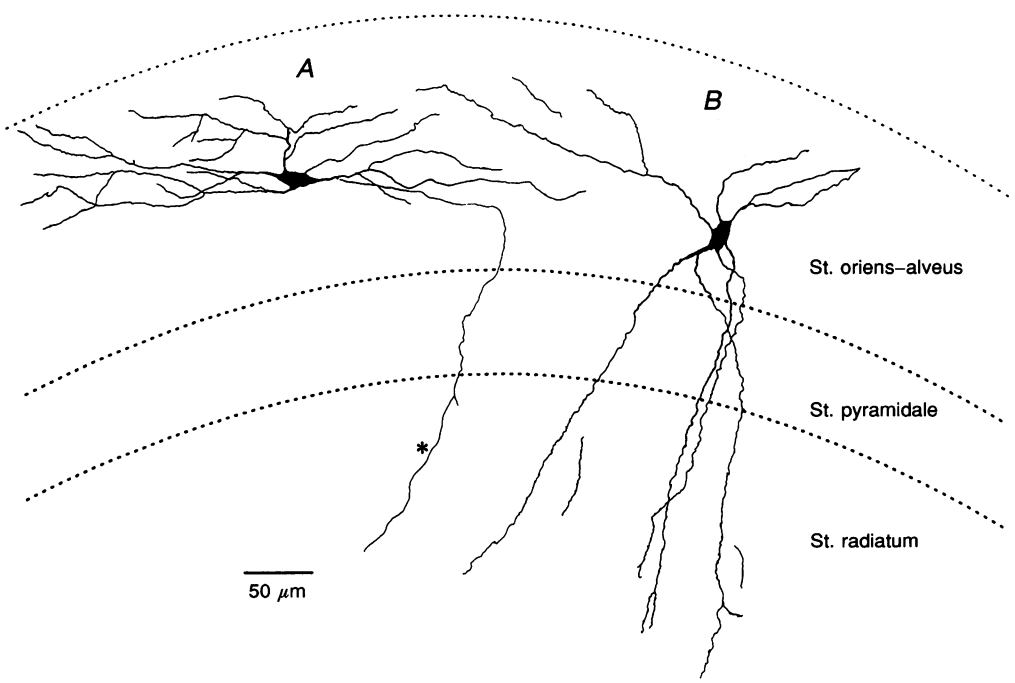

Figure 1. Morphological properties of st. O–A interneurones

Camera lucida reconstruction of two representative inhibitory interneurones of st. O–A. The cells were filled with biocytin during whole-cell recording prior to excision of the outside-out patch. Slices were then fixed and processed for the biocytin staining. Cells were reconstructed from 5 × 50 μm-thick sections using camera lucida techniques. Two main cell types were identified based on their morphological properties. The cell soma of both were multipolar and gave rise to dendrites that were either oriented parallel to the alveus (horizontal st. O–A interneurones; *A*), or traversed st. pyramidale into st. radiatum and lacunosum–moleculare (*B*). The axon of the horizontal interneurone, indicated by an asterisk, typically crossed over the st. pyramidale and radiatum to terminate in the st. lacunosum–moleculare. Axons of the vertically oriented cell were restricted to the pyramidal cell layer (not shown).

conditioning hyperpolarizing pulse (−90 mV for 100 ms), outward currents were comprised of a rapidly activating transient current component followed by a non-inactivating sustained current (Fig. 2). Point by point subtraction of the two current families allowed the resolution of a current component which activated and inactivated rapidly, with a phenotype resembling the traditional transient A-current of most neurones (Connor & Stevens, 1971; $n = 12$). Such a manipulation was used to isolate the rapid activating transient component of the outward current throughout this study.

Ionic selectivity of the outward currents

The ionic selectivites of the outward currents in st. O–A cells were analysed using tail currents elicited following a 100 ms depolarizing step. At this time point, tail currents were assumed to arise primarily from the sustained current. The amplitude and the polarity of the tail currents produced should depend on the difference between the test potential and the equilibrium potential for K^+ if the outward current is carried exclusively by potassium ions. Following a depolarization to +20 mV from a holding potential of −60 mV, return of the membrane potential to various test potentials (−40 to −110 mV) produced a family of tail currents. As shown in Fig. 3, the polarity and amplitude of the peak tail currents were dependent on the test voltages and on $[K^+]_o$. With 3·5 mM K_o^+ and 140 mM K_i^+, the tail currents reversed polarity at −93·2 ± 1·3 mV ($n = 4$) in outside-out patches and −92·0 ± 1·5 mV ($n = 5$) in whole-cell recordings. These values are close to the predicted equilibrium potential of K^+ (−95 mV) as calculated by the Nernst equation. To determine the ionic selectivity of the tail current, we increased the $[K^+]_o$ from 3·5 to 10 and 20 mM. In 10 mM K_o^+ the reversal potential was shifted to −68·5 ± 1·2 mV ($n = 4$) in outside-out patches and −70·0 ± 1·4 mV ($n = 5$) in whole-cell recordings. In 20 mM K_o^+ the reversal potential was −51·0 ± 1·4 mV ($n = 4$) from outside-out patches and −53 ± 1·5 mV in whole-cell recordings ($n = 5$) (Fig. 3). Plots of the predicted reversal potentials and experimental data show close overlap (Fig. 3*C*). To examine the ionic selectivity of the transient current we repeated the above

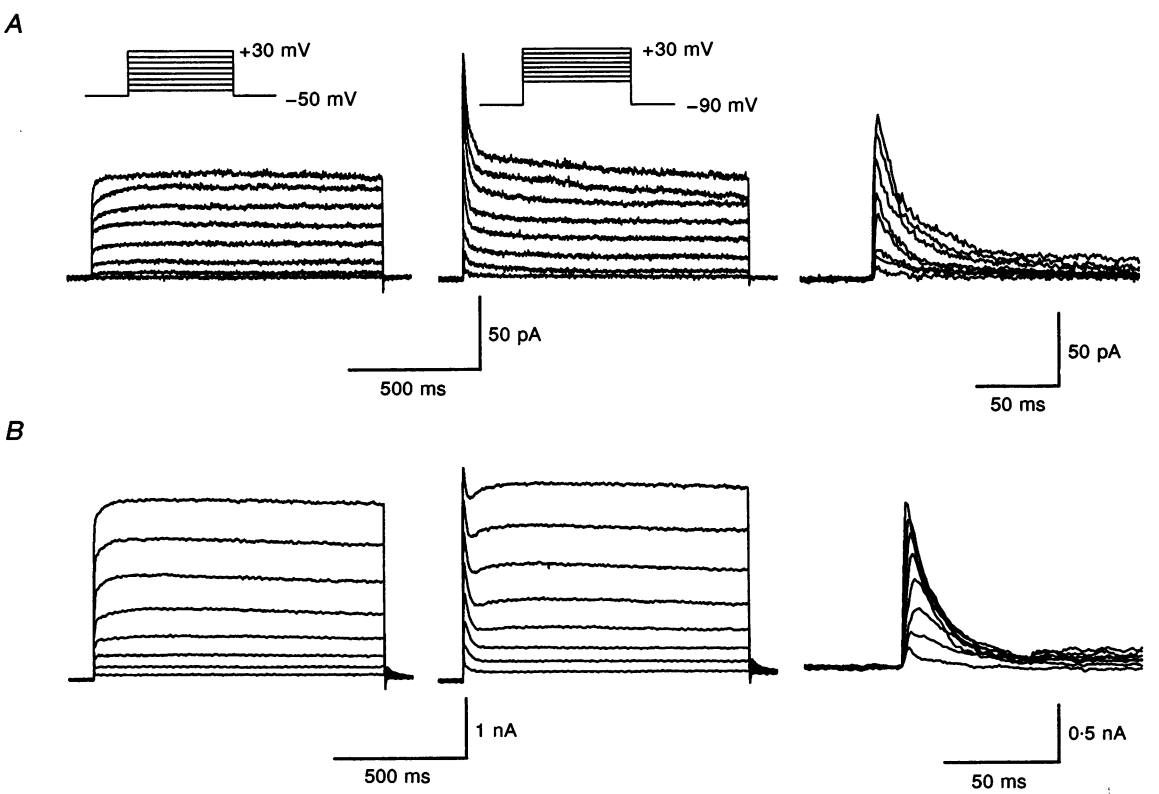

Figure 2. Outward currents of hippocampal inhibitory interneurones

Typical outward currents obtained from either outside-out patch (*A*) or whole-cell configuration (*B*). Currents elicited by depolarization steps from a holding potential of −50 mV consisted solely of a sustained component, while currents from a holding potential of −90 mV comprised both a transient and a sustained component. Digital subtraction of the family elicited from a holding potential of −50 mV from that elicited from −90 mV permitted the isolation of the transient current component (right column). The isolated transient current obtained from either outside-out patches or whole-cell recordings shared identical properties, demonstrating that the channel properties were not altered during excision of the outside-out patch.

experiments using short (5 ms) depolarizing pulses to elicit predominantly the transient current component. With 3·5 mM K_o^+ and 140 mM K_i^+, tail currents reversed polarity at $-89 \pm 1{\cdot}3$ mV ($n = 5$). In 8·5 mM K_o^+ the tail currents reversed polarity at $-69 \pm 0{\cdot}6$ mV ($n = 3$). This value is close to the predicted shift in the reversal potential (+23 mV). These experiments suggested that both outward current components in st. O–A cells were carried primarily by K^+ ions.

Voltage dependence and kinetic properties of the transient K^+ current, I_A

We considered that during excision of the outside-out patch, a loss of N-type inactivation of the channels underlying the transient current may occur due to cysteine oxidation (Ruppersberg, Stocker, Pongs, Heinemann, Frank & Koenen, 1991). To prevent this, this series of experiments were performed using an intracellular solution containing glutathione (5 mM). In addition Mg^{2+} was omitted from the internal solution to remove any possible block of I_A by Mg^{2+} at extreme positive potentials.

The isolated I_A reached a peak current within 5 ms following the onset of membrane depolarization. The current activation was followed by rapid inactivation or decay of the current despite a continued membrane depolarization (Fig. 4*A*). This inactivation was best fitted by a monoexponential function whose rate showed little or no voltage dependence. The time constants for the inactivation upon depolarization to 0 and +20 mV from a holding potential of −90 mV were $16{\cdot}1 \pm 1{\cdot}8$ and $17{\cdot}7 \pm 1{\cdot}9$ ms ($n = 5$), respectively. Plots of the voltage dependence of I_A activation were constructed by dividing the peak current by the current driving force ($V_{test} - V_r$), where V_{test} was the step depolarization potential and V_r was the reversal potential (Fig. 4*C*). The activation profiles were fitted with a Boltzmann equation of the form:

$$g/g_{max} = [1 + \exp\{(V_{½} - V)/V_c\}]^{-1},$$

where g/g_{max} is the conductance normalized to its maximum value, V is the membrane potential, $V_{½}$ is the membrane voltage at which the current amplitude is half-maximum and V_c is a constant. The Boltzmann isotherm for inactivation has the form:

$$I/I_{max} = [1 + \exp\{(V_{½} - V)/V_c\}]^{-1},$$

where I/I_{max} is the current amplitude normalized to its

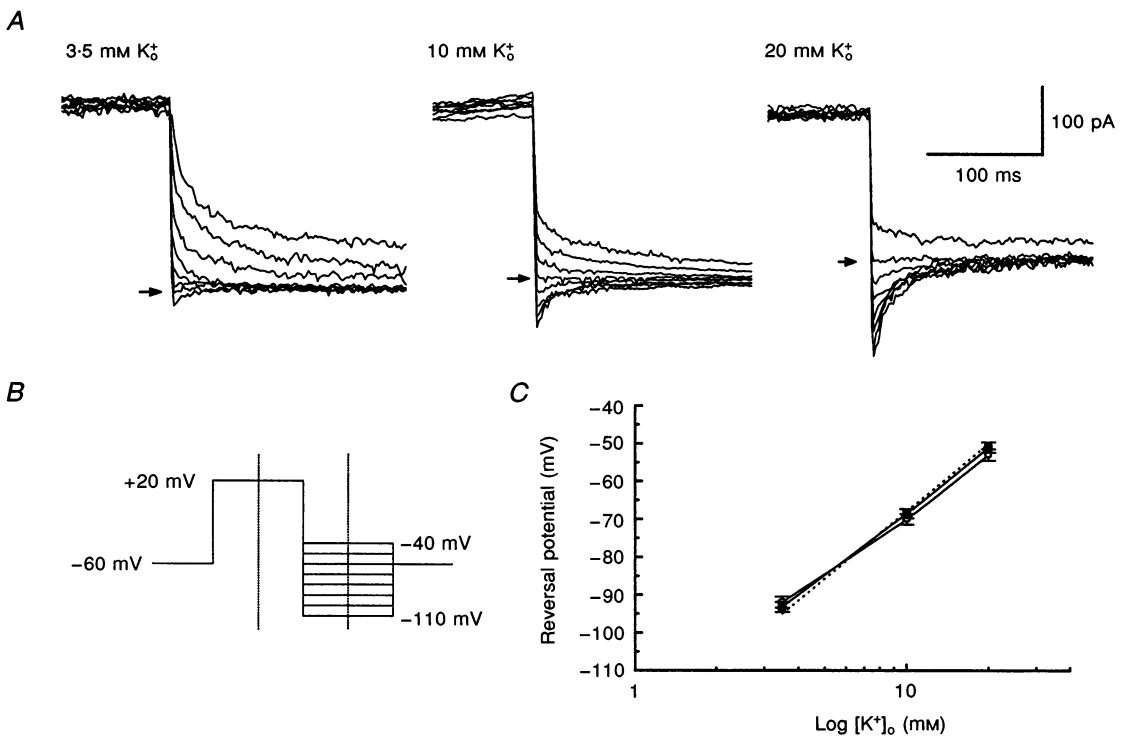

Figure 3. Ionic selectivity of the outward currents in outside-out patches

Following a depolarization to +20 mV (100 ms duration) to activate the outward currents, the membrane potential was returned to various potentials (from −110 to −40 mV) to elicit tail currents. The amplitude and direction of the tail currents varied with both the driving force and the $[K^+]_o$ (*A*). The arrows indicate the potential at which zero current flowed (i.e. the current reversal potential). Only the currents elicited within the dotted lines of the experimental step protocol are shown (*B*). *C*, a plot of the experimentally measured reversal potentials against the logarithm of $[K^+]_o$ obtained from both outside-out patches (■) and whole cells (○) showed close agreement with the plot of predicted reversal potentials as calculated from the Nernst equation (dashed line).

maximum value. A fit of the data with the Boltzman isotherm revealed a half-activation ($V_{½}$) of −18·6 ± 2·3 mV (Fig. 4*C*). The slope (V_c) of the activation curve was 16·6 ± 1·5 mV. In a small number of outside-out patches, a second type of transient current was observed which activated at potentials close to −35 mV, with half-activation at +9·9 ± 0·9 mV with a slope of 7·8 mV ($n = 4$, data not shown). Due to its low frequency of occurrence, this current type was not studied further.

The properties of I_A were not altered when studied under whole-cell or outside-out configuration (Fig. 2). In whole-cell recordings the time constants for the inactivation of I_A at test potentials of +20 and −10 mV were 19·1 ± 4·2 ms ($n = 6$) and 21·5 ± 3·9 ms ($n = 8$), respectively. The half-activation and half-inactivation potentials were −14·4 ± 2·2 mV ($n = 14$) and −74·4 ± 0·7 mV ($n = 7$), respectively. These values are very close to those obtained in outside-out patches suggesting that I_A in outside-out patches accurately represents the transient current of the whole cell.

Identical data were obtained when glutathione was omitted and Mg^{2+} (1 mM) was added to the internal solution

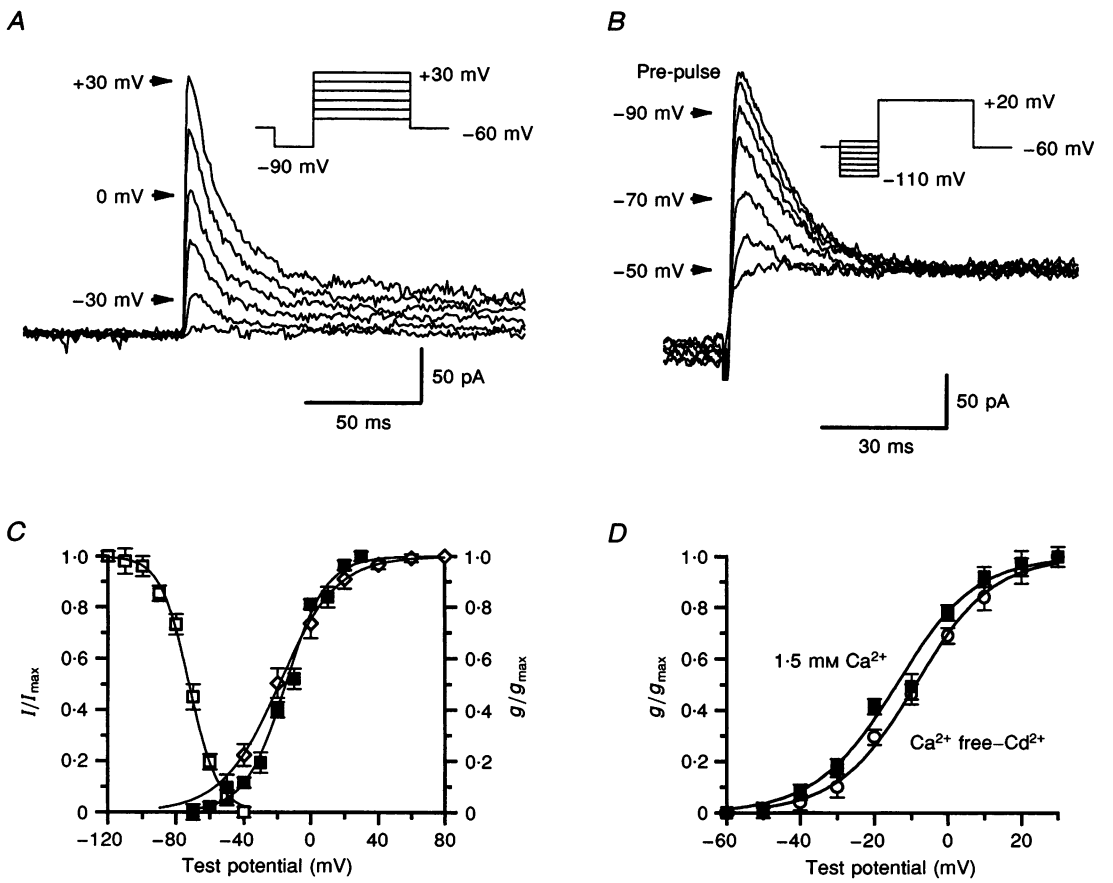

Figure 4. The voltage dependence and kinetic properties of the transient current component measured in outside-out patches

The transient current in isolation was activated within 5 ms after the onset of the depolarizing step and inactivated rapidly with a time constant of approximately 15 ms at a test potential of 0 mV (*A*). *B*, the activation of the transient current was strongly affected by the prepulse potentials delivered prior to current activation. A pre-pulse (100 ms duration) to progressively more positive potentials resulted in a decrease in the amplitude of the transient current evoked by a fixed depolarization to +20 mV. *C*, the voltage-dependent activation (◇) and inactivation (□) curves of the transient current component. In these experiments the voltage dependence of activation was determined using either an intracellular solution containing glutathione (10 mM) in which Mg^{2+} was omitted, or alternatively a solution containing no glutathione and with 1 mM Mg^{2+} added (■). Identical data were obtained in recordings made with both intracellular solutions. The transient current activated at potentials positive to −80 mV, and was completely inactivated at potentials close to −40 mV. The membrane potentials at which half-activation and half-inactivation occurred were −18 mV (◇) or −14·4 mV (■) and −72 mV (□), respectively. *D*, the voltage dependence of activation of the transient current (■, control) was shifted 5 mV to the right in Ca^{2+}-free, Cd^{2+} (0·1 mM)-containing solutions (○).

($V_{½} = -14{\cdot}4 \pm 1{\cdot}2$ mV, $V_c = 13{\cdot}8 \pm 2{\cdot}3$, $n = 14$; Fig. 4*C*). Likewise the time constants for the inactivation upon depolarization to 0 and +20 mV from a holding potential of −90 mV were $15{\cdot}1 \pm 1{\cdot}4$ and $16{\cdot}6 \pm 0{\cdot}9$ ms ($n = 6$), respectively.

Voltage-dependent inactivation of I_A

The voltage-dependent inactivation of I_A was studied using depolarizing steps to a fixed voltage (+20 mV) preceded by a series of prepulse conditioning potentials ranging from −120 to −40 mV (100 ms; Fig. 4*B*). I_A was completely inactivated at prepulse potentials positive to −40 mV. As the prepulse potential was made progressively more negative, the amplitude of I_A increased. The relative amplitudes of the currents were plotted, and fitted with a Boltzman equation to generate an inactivation curve (Fig. 4*C*). Half-inactivation of I_A occurred at $-71{\cdot}9 \pm 3{\cdot}2$ mV with a slope factor of $-7{\cdot}3 \pm 0{\cdot}8$ mV ($n = 7$). The activation and inactivation curves overlapped such that I_A produced a window current between −40 and −80 mV with a maximum around −58 mV (Fig. 4*C*).

The voltage dependence and kinetics of I_A activation were dependent on the external divalent ion concentration. In outside-out patches perfused with a Ca^{2+}-free, Cd^{2+}-containing (100 μM) solution, both the peak amplitude and the inactivation time constant were decreased compared with control ($Ca^{2+} = 1{\cdot}5$ mM; Fig. 4*D*). At a test potential of +10 mV, the time constant for current inactivation was $11{\cdot}0 \pm 0{\cdot}2$ ms in Ca^{2+}-free, Cd^{2+}-containing solution and $14{\cdot}7 \pm 0{\cdot}3$ ms in normal $[Ca^{2+}]_o$ ($n = 4$, $P < 0{\cdot}01$). Furthermore, as shown in Fig. 4*D*, Cd^{2+}-containing

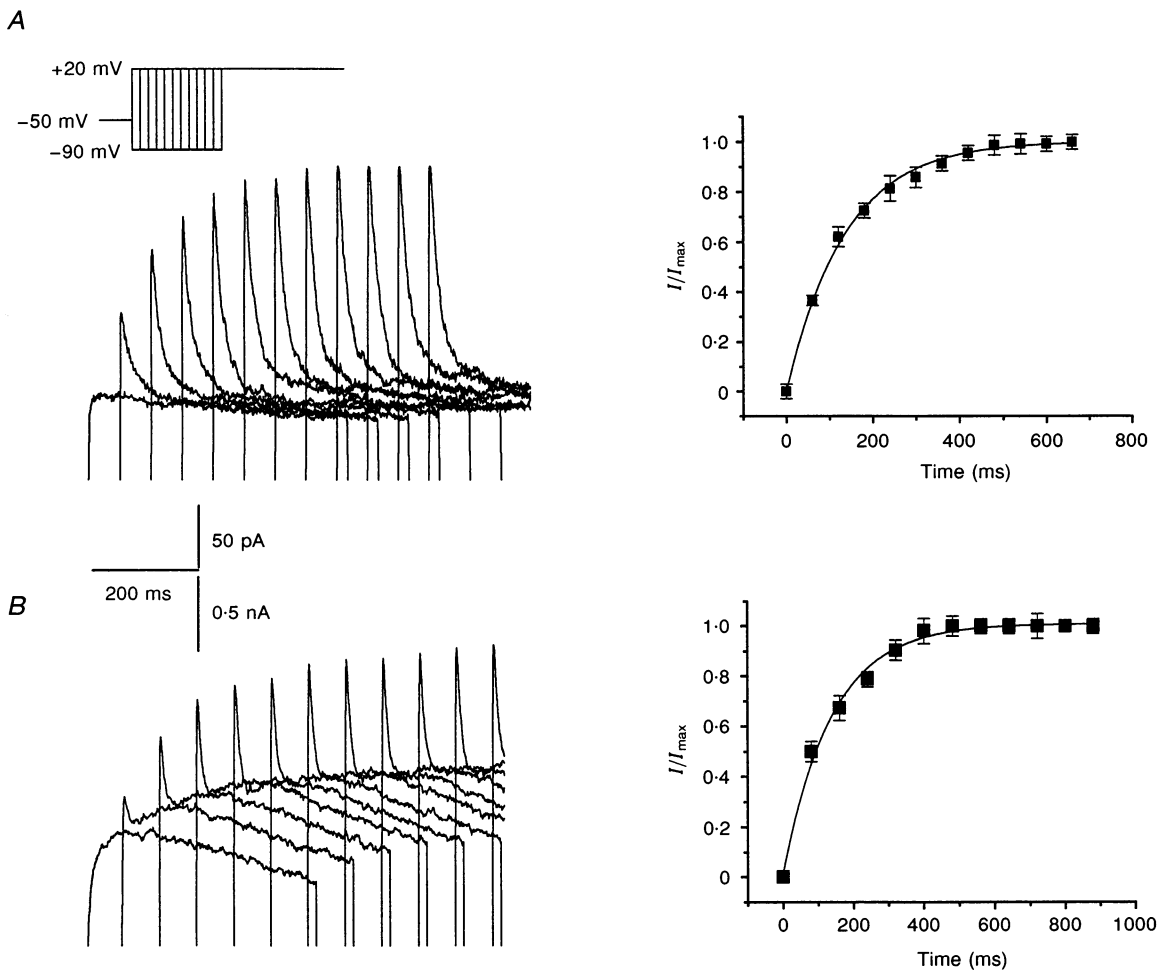

Figure 5. The time-dependent recovery from inactivation of the transient current in outside-out patches (*A*) and whole-cell recordings (*B*)

Currents were evoked by a fixed depolarization to +20 mV following a pre-pulse to −90 mV for varying durations (0–900 ms) from a holding potential of −50 mV. The amplitudes of the peak transient currents were normalized to the maximum elicited transient current and plotted against the pre-pulse duration. The rate of recovery from inactivation was described by a single exponential with a time constant of $142{\cdot}3 \pm 7{\cdot}8$ ms in outside-out patches and $134{\cdot}6 \pm 5{\cdot}3$ ms in the whole-cell recordings. Data points represent the means of 6 patches and 9 whole-cell recordings. Currents were recorded in the presence of 1–5 mM TEA to permit the isolation of the transient current component.

solutions shifted the voltage dependence of I_A activation to more positive potentials. The half-activation of I_A in Ca^{2+}-containing or Ca^{2+}-free, Cd^{2+}-containing solution were −14·3 and −9·0 mV, respectively ($n = 4$).

Time-dependent removal of inactivation of I_A

Outside-out patches were held at −50 mV to inactivate I_A, and the membrane potential was then stepped to −90 mV for periods between 0 to 900 ms to deinactivate I_A prior to a test pulse to +20 mV. Figure 5 shows representative records of the time-dependent recovery from inactivation of I_A in both outside-out patches and whole-cell recordings. Normalized peak I_A was plotted against prepulse duration to reveal the time course of recovery from inactivation. The recovery from inactivation was fitted by a single exponential function with a time constant of 142·3 ± 7·8 ms in outside-out patches ($n = 6$) and 134·6 ± 5·3 ms in whole-cell recordings ($n = 9$; Fig. 5).

Sustained current component, I_K

At a holding potential of −50 mV, a voltage where I_A is >90% inactivated, depolarizing steps to potentials greater than −40 mV elicited currents that activated relatively slowly and showed little time-dependent inactivation during a 1 s depolarizing step (Fig. 6). A large part of the sustained current was found to be dependent on extracellular Ca^{2+}. In Ca^{2+}-free, Cd^{2+}-containing solutions (0·1 mM) the amplitude of the outward current was markedly reduced, presumably by preventing Ca^{2+} influx and consequent activation of Ca^{2+}-activated potassium

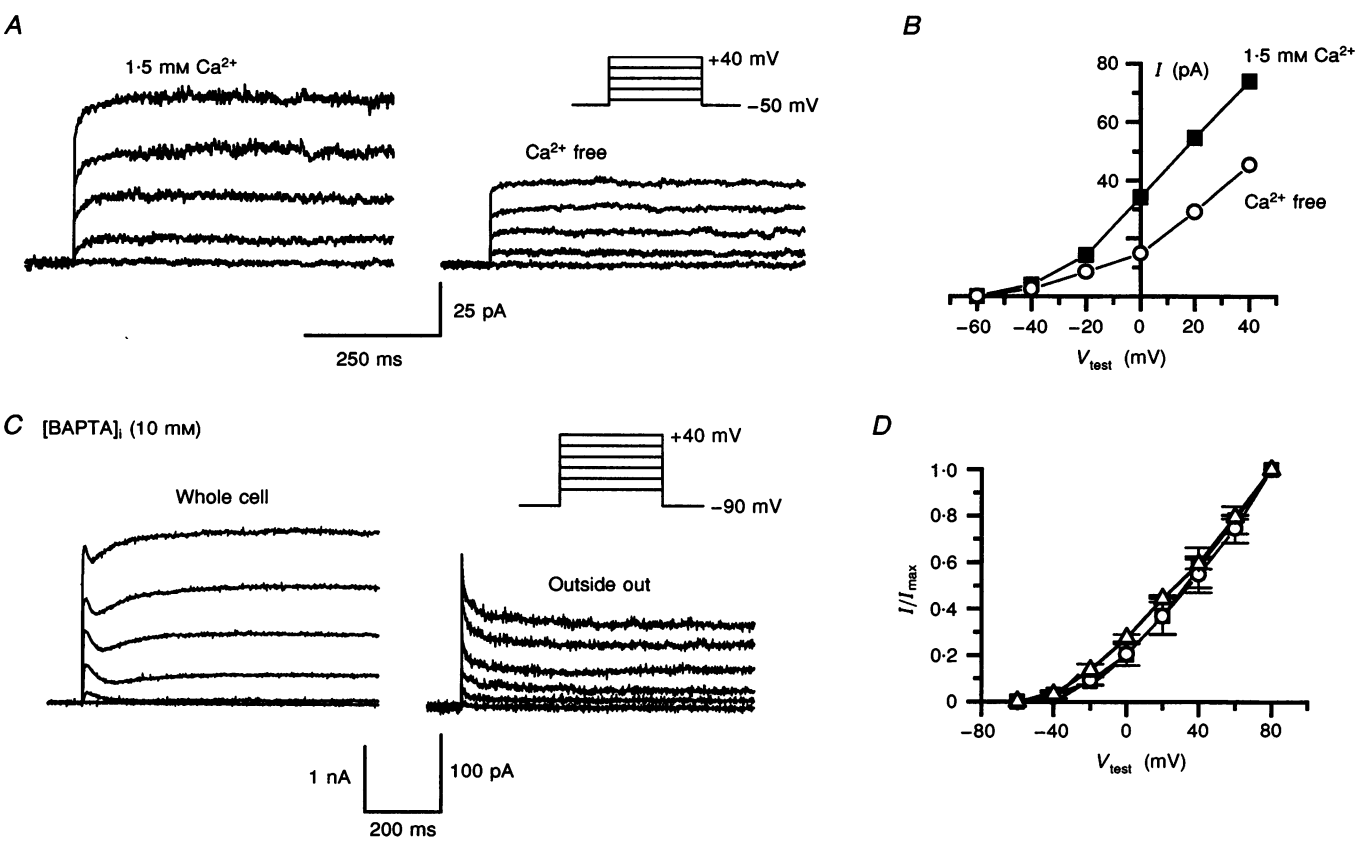

Figure 6. The sustained outward current comprises both a Ca^{2+}-dependent and -independent component

A, sustained outward current families were recorded in an outside-out patch from a holding potential of −50 mV to various test potentials (see inset) when bathed in either normal ACSF containing 1·5 mM Ca^{2+} or Ca^{2+}-free ACSF containing 0·1 mM Cd^{2+}. *B*, the voltage–current plots of the isolated current components of the data illustrated in *A* show that in Ca^{2+}-free ACSF the current is markedly attenuated. Both currents, however, activated at potentials close to −40 mV and possessed similar voltage–current relationships. *C*, in another series of experiments the sustained current was measured in a whole-cell recording (left panel) prior to the excision of the outside-out patch (middle panel) using electrodes filled with an internal solution to which 10 mM BAPTA had been added. The data from both recording configurations possessed both transient and sustained current components. *D*, sustained current data obtained under three recording conditions, control (1·5 mM Ca_o^{2+}, ■), Ca^{2+}-free, Cd^{2+}-containing solution (○) or 10 mM $BAPTA_i$ (△) were normalized and the voltage–current data plotted. The families of sustained currents obtained in these three experimental conditions showed almost complete overlapping properties.

conductances (Fig. 6A). At 0 mV, the total outward currents were reduced by 44·1 ± 4% ($n = 8$; Fig. 6B) in the Ca^{2+}-free, Cd^{2+} containing solution. Isolation of the Ca^{2+}-dependent component by digital subtraction of the current obtained in the presence and absence of Ca^{2+}-containing solutions revealed a current that was activated at potentials positive to −30 mV, which did not inactivate during a 1 s depolarizing step ($n = 5$). Alternatively, the sustained current component was studied in isolation by inclusion of 10 mM BAPTA in the intracellular solution (Fig. 6C). A comparison of the voltage–current plots of I_K revealed no difference in the properties of this current component when measured in Ca^{2+}-free conditions or using intracellular BAPTA (Fig. 6D, $n = 11$). A similar current component could be isolated in the presence of iberiotoxin (100 nM, data not shown, $n = 4$), derived from scorpion venom, which selectively blocks large conductance Ca^{2+}-activated K^+ channels (Candia, Garcia & Latorre, 1992).

Tail currents evoked at −30 mV, from a test potential of +20 mV, were fitted by multiple exponentials the number of which was dependent on the $[Ca^{2+}]_o$. In Ca^{2+}-containing solutions, tail currents were best described by three exponentials of 9·0 ± 3·3, 27·6 ± 4·9 and 93·4 ± 13·6 ms ($n = 6$). In Ca^{2+}-free, Cd^{2+}-containing solutions the tail currents were best fitted by two exponential functions, 6·9 ± 1·2 and 25·7 ± 4·1 ms ($n = 9$). The third longer duration decay time constant was absent in these Ca^{2+}-free conditions. These data suggest that at least two, possibly three, sustained currents comprise the total sustained outward current of st. O–A interneurones. This slowly deactivating current component was not studied further and, in order to minimize the Ca^{2+}-activated K^+ conductance, all sustained currents were subsequently studied in Ca^{2+}-free solution.

Figure 7 illustrates the voltage-dependent activation profile of the sustained current elicited by a series of depolarizing potentials from a holding potential of −50 mV. In contrast to the transient current, this sustained current activated more slowly in response to a depolarizing step. At +20 mV, the time for the current to attain maximum amplitude was 83·2 ± 10·5 ms in outside-out patches ($n = 8$). Despite the relatively slow time-to-current peak, it was observed that at 1·5 ms following the step depolarization (V_{test}, +20 mV), 81·8 ± 2·7% of the peak amplitude was attained in outside-out patches ($n = 11$). Similar data were obtained in whole-cell recordings (77·1 ± 4·9% of maximum current amplitude, $n = 9$). The lack of saturation of the sustained current at positive voltages did not permit an analysis of the voltage-dependent activation properties of this current (Fig. 7C). In contrast to the transient current, sustained currents showed no voltage-dependent inactivation over a wide range of test voltages (−120 and −40 mV; Fig. 7B and C).

Though the majority of cells possessed an I_K which did not inactivate during 1 s depolarization steps, approximately 20% of sustained currents demonstrated some time-dependent inactivation (cf. currents in Figs 2 and 9). These slow-inactivating currents elicited at 0 and +30 mV decayed monoexponentially with a time constant of 1·9 ± 0·1 and 2·2 ± 0·1 s, respectively ($n = 6$) and occurred predominantly in whole-cell recordings. In five

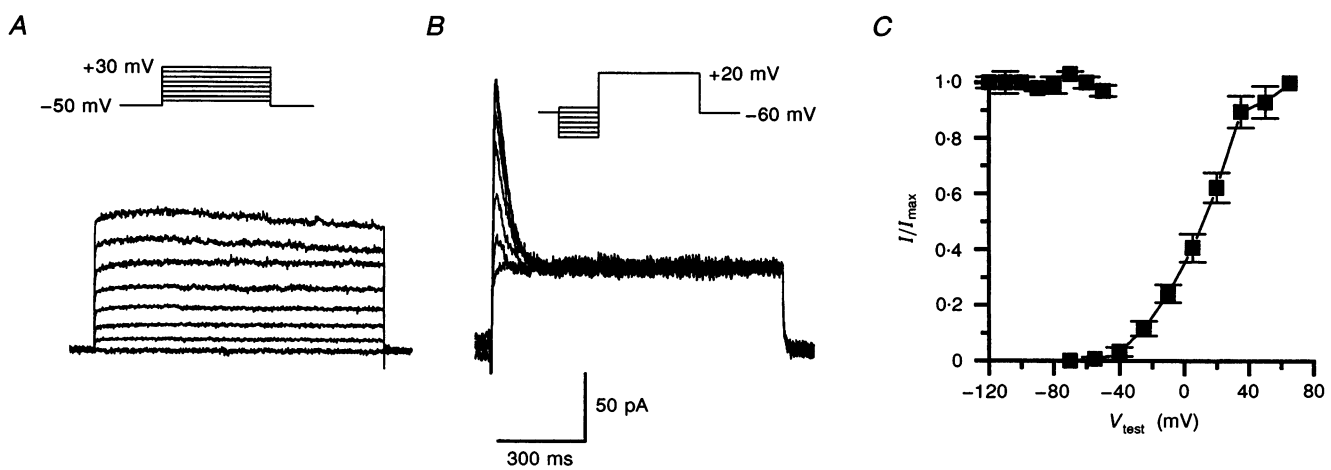

Figure 7. Voltage-dependent and kinetic properties of the Ca^{2+}-independent sustained outward current

In outside-out patches current families were elicited by depolarization steps from a holding potential of −50 mV to the test potentials shown in the insets. Depolarizing steps were delivered in 10 mV increments. The activated currents showed little time-dependent inactivation during a 1 s depolarization step (A). The sustained current component has no voltage-dependent inactivation. The amplitude of the sustained currents when depolarized to +20 mV was not affected by the pre-pulse potential (100 ms) (B). C, summarized plots of the voltage-dependent activation and inactivation properties of the Ca^{2+}-independent sustained currents. All data were recorded in a Ca^{2+}-free, Cd^{2+} (0·1 mM)-containing solution.

cells, the time course of this slow time-dependent inactivation was studied using a 5 s depolarization voltage step ($V_{test} = 0$ mV). During this test pulse the time-dependent inactivation of the current could be fitted by a single exponential with a time constant of $2{\cdot}4 \pm 0{\cdot}3$ s ($n = 5$).

Pharmacology of the outward currents

We next studied the effects of the potassium channel antagonists 4-AP and TEA on both I_A and I_K current components. 4-AP is a K^+ channel blocker known to selectively inhibit I_A in many preparations (Thompson, 1977; Gustafsson, Galvan, Grafe & Wigström, 1982; Numann *et al.* 1987; Ficker & Heinemann, 1992). In Ca^{2+}-free, Cd^{2+}-containing solution, 4-AP selectively blocked I_A with an IC_{50} of 1·7 mM (Fig. 8; $n = 12$). The subtraction currents obtained from records before and during high concentrations of 4-AP (Fig. 8) resembled those generated by the subtraction of the outward currents evoked from holding potentials of −90 or −50 mV as shown in Fig. 2*A*. Low concentrations of 4-AP also attenuated the peak amplitude of I_K. At 0 mV, 4-AP (50 μM) reduced the amplitude of I_K by $12{\cdot}2 + 1{\cdot}1$% ($n = 5$). 4-AP was without further effect on I_K component at concentrations of up to 10 mM ($n = 8$).

Dendrotoxin

Dendrotoxin (DTX) has been shown to block a slowly inactivating transient current in a variety of preparations (Halliwell, Othman, Pelchen-Mathews & Dolly, 1986). Recently DTX has been shown to selectively block current through channels formed by a variety of members of the *Shaker* subfamily of potassium channels (Stuhmer *et al.* 1989). In the present experiments DTX was added in concentrations of up to 0·5 μM. At these concentrations DTX was without effect on any of the current components recorded in these cells ($n = 4$, data not shown). Prior treatment of the perfusion system and recording chamber with 0·1% BSA in order to avoid unspecific adsorption of DTX yielded identical data ($n = 3$).

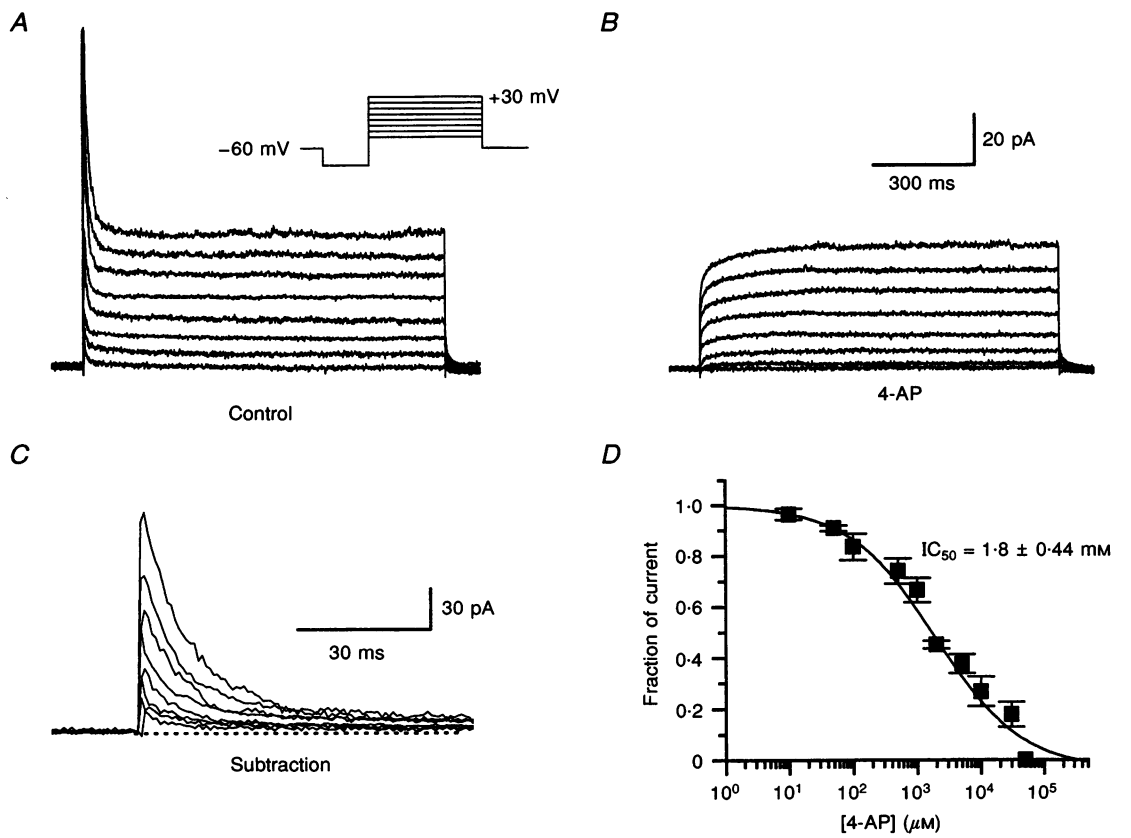

Figure 8. 4-AP selectively blocks I_A

Currents were evoked by depolarizing steps following a pre-pulse potential to −90 mV to deinactivate the transient current, as shown in the inset (*A*). Addition 4-AP (5 mM) blocked the transient current and reduced the amplitude of the sustained currents by ~10% (*B*). *C*, at each concentration the family of currents obtained in the presence of 4-AP was subtracted from the control family to allow the isolation of that fraction of current blocked by 4-AP. In this panel data are shown for the transient component blocked by 5 mM 4-AP. *D*, a dose–response curve for the block of the transient current by 4-AP. Each point represents the mean data obtained from 4 to 12 cells. Data were fitted with the logistic equation $I/I_{max} = 1/(1 + ([4\text{-AP}]/IC_{50})^n)$. 4-AP blocked I_A with an IC_{50} of $1{\cdot}8 \pm 0{\cdot}44$ mM.

Tetraethylammonium

TEA has been used to block a variety of voltage-dependent and Ca^{2+}-activated potassium currents in a number of central neurones. In order to study the effects of TEA block on I_K, cells were held at −50 mV and perfused in Ca^{2+}-free, Cd^{2+}-containing solution to minimize Ca^{2+}-activated and transient conductances. TEA (1–30 mM) suppressed I_K in a dose-dependent manner (Fig. 9). TEA did not affect the activation threshold or voltage dependence of I_K but clearly diminished the peak amplitude (Fig. 9*B*). At a test potential of 0 mV, TEA reversibly reduced the maximal amplitude of I_K by 16·4, 35·8 and 73·7% at a concentration of 1, 5 and 20 mM, respectively ($n = 6$). The apparent IC_{50} of TEA block of I_K occurred at 7·4 ± 0·7 mM (Fig. 9*C*). In three outside-out patches TEA (5 mM) reduced the peak amplitude of the transient current component activated from a holding potential of −90 mV by only ~5% ($n = 3$, data not shown). Since I_A was not studied in isolation in these outside-out-patches it is unclear whether this reduction reflects the effects of TEA on the overlapping I_K component.

DISCUSSION

Here we have characterized three main phenotypes of voltage-dependent K^+ current present in st.O–A interneurones of the CA1 hippocampus. The use of outside-out patches excised from the cell soma has permitted the analysis of the voltage-dependent properties of these currents free from the space-clamp or series resistance errors usually associated with whole-cell recordings of interneurones in the *in vitro* slice preparation (Thurbon *et al.* 1994). The majority of patches excised from these cells contained a sufficient number of channels to allow analysis of macroscopic K^+ currents from morphologically characterized interneurones. Such a recording configuration not only allows a more accurate determination of the properties of currents of morphologically identified interneurones from the *in vitro* slice preparation but circumvents the necessity of acutely isolating or placing into primary culture cells of interest. In a number of experiments we were able to obtain data from both whole-cell and outside-out patches in a single cell. On these occasions it was observed that the K^+ current properties

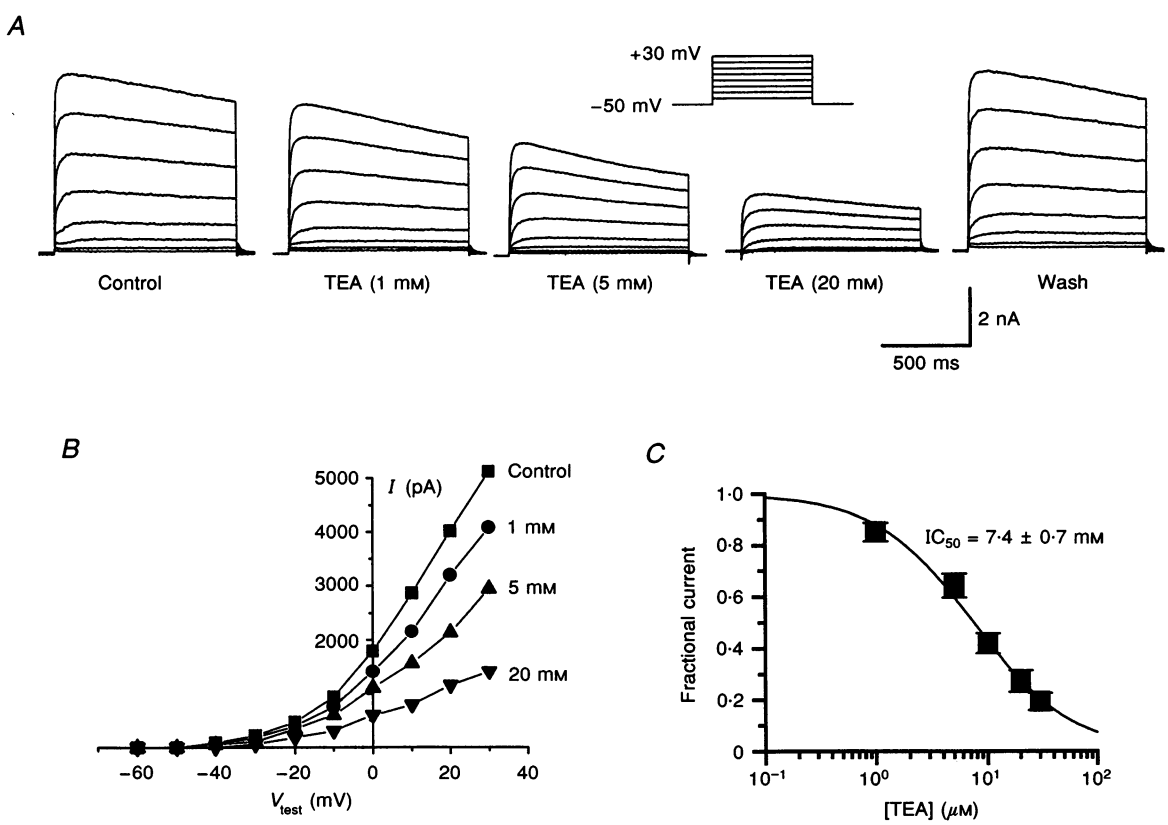

Figure 9. TEA selectively blocks the sustained current component

Externally applied TEA (1–20 mM) reversibly inhibited the sustained currents evoked by depolarizations from a holding potential of −50 mV in a representative whole-cell recording (*A*). *B*, the current–voltage relationships in the presence of increasing concentrations of TEA obtained from the current families shown in *A*. V_{test}, step-depolarizing potential. *C*, a dose–response curve for the block of the sustained current by TEA. Each point represents the mean data obtained from 8 cells. Data were fitted with the logistic equation $I/I_{max} = 1/(1 + ([TEA]/IC_{50})^n)$. TEA blocked I_K with an IC_{50} of 7·4 ± 0·7 mM.

were not markedly altered in the formation of the outside-out patch (cf. Ruppersberg, Ermler, Knopf, Kues, Jonas & Koenen, 1993). Often the ratio of the transient to sustained current component differed in the patch from that seen in whole-cell configuration. This observation is due either to the differing numbers of 'transient' *versus* 'sustained' channels included during the formation of the patch, or alternatively it may reflect the differential distribution of these channels across the somato-dendritic axis. We tend to favour the former hypothesis, since we were able to observe both current components in virtually all patches from which recordings were made.

St. O–A cells, like most central neurones, possess both a transient, rapidly inactivating current, I_A, and at least two sustained 'delayed-rectifier' I_K current phenotypes. The time to peak, rate of inactivation, voltage dependence and rate of recovery from inactivation are similar to the I_A of pyramidal cells (Numann *et al.* 1987; Ficker & Heinemann, 1992). The voltage dependence of I_A activation was shifted to the right in Ca^{2+}-free, Cd^{2+}-containing solutions consistent with the observations of Talukder & Harrison (1995) in cultured hippocampal cells. The similarity of I_A in st. O–A cells and pyramidal cells suggests that these currents may arise from identical K^+ channel subunit expression.

Information on K^+ channel subunit mRNA expression patterns in the various hippocampal interneurone populations is largely incomplete, making the correlation of the subunit expression patterns with the current properties of st. O–A cells difficult. To date, five members of the mammalian *Sh* K^+ channel family have been shown to encode channels with a transient current phenotype: Kv1.4, Kv3.3, Kv3.4, Kv4.1 and Kv4.2. Based on their voltage dependence of activation and inactivation, time constant of inactivation and sensitivity to 4-AP in the millimolar range, only two of these K^+ channel subunits are likely to be constituents of the channels underlying I_A in st. O–A cells, namely Kv4.1 and Kv4.2 (for review see Pongs, 1992). Recent evidence suggests that channels formed from these subunits underlie the low threshold, transient A-current, I_{SA}, in *Xenopus* oocytes injected with whole rat brain RNA (Serodio, Kentros & Rudy, 1994). In the hippocampus both CA1 and CA3 pyramidal neurones show high levels of Kv4.2 mRNA expression, consistent with the properties of the A-type currents in the pyramidal neurones. At this time, however, it is not known if interneurones of the hippocampus express this mRNA transcript in similarly abundant levels.

Antibodies raised against Kv1.4 have shown that this subunit's expression in the hippocampus is restricted to interneurones located close to the pyramidal cell layer (Rettig *et al.* 1992). It is unlikely, however, that channels formed by this subunit underlie the transient current in st. O–A cells for several reasons. First the recovery from inactivation of Kv1.4 channels is in the range of seconds (Ruppersberg *et al.* 1991), while the transient current in st. O–A cells recovered from inactivation with a time constant close to 140 ms. Secondly, excision of inside-out patches containing these channels is known to result in a loss of current inactivation, by a mechanism involving cysteine oxidation (Ruppersberg *et al.* 1991). Inactivation can be restored by exposure of the patch to glutathione. In the present experiments I_A was always observed, whether glutathione was present or absent from the intracellular solution. Finally, the interneurones from which these recordings were made were located at the border of the st. oriens and alveus, an area where protein expression of Kv1.4 was absent.

A small percentage (~20%) of transient currents had properties distinct from the predominant I_A phenotype. These currents activated at more positive potentials ($V_{½} \approx +10$ mV). In addition, transient currents in two of the three outside-out patches possessed time constants of inactivation which were strongly voltage dependent (C. J. McBain, unpublished observation). These currents are reminiscent of those encoded by members of the *Shaw* subfamily, Kv3.3 and Kv3.4 (Vega-Saenz de Miera, Moreno, Fruhling, Kentros & Rudy, 1992; Weiser *et al.* 1994). Both Kv3.3. and Kv3.4 activate at positive potentials and are blocked by low concentrations of TEA and 4-AP. *In situ* hybridization studies have shown that Kv3.3, but not Kv3.4, is expressed in extremely low levels in the hippocampus in cells tentatively identified as interneurones of st. radiatum, pyramidale and oriens. It remains to be determined whether the positively activating I_A results from channels formed by members of the *Shaw* subfamily.

The sustained current I_K observed in st. O–A neurones showed virtually no inactivation over a wide range of voltages and showed minimal time-dependent inactivation. This is in marked contrast to the 'delayed rectifier' described in both cultured and acutely dissociated pyramidal neurones, which shows marked inactivation at voltages close to the resting membrane potential as well as marked time-dependent inactivation (Numann *et al.* 1987; Ficker & Heinemann, 1992). The sustained current of st. O–A cells activated rapidly, such that > 80% of the total current was activated by 1·5 ms. This is in contrast to pyramidal neurones, which require > 100 ms for complete activation (Numann *et al.* 1987). A lack of voltage- and time-dependent inactivation of I_K is likely to have important consequences for st. O–A cells during sustained repetitive firing. These channels will ensure adequate spike repolarization occurs without an accumulation of inactivation of these channels during prolonged episodes of action potential activity common to these cells. In the accompanying current clamp study we determine the role of this current during action potential firing.

The molecular identity of the K^+ channel subunits underlying I_K in st. O–A cells is at present unclear. Both

Kv1.1 and Kv1.2 mRNAs are known to be widely expressed in the mature hippocampus (Kues & Wunder, 1992). These subunits are extremely sensitive to block by DTX ($IC_{50} \approx 20$ nM; Grissmer *et al.* 1994). Their mRNA expression pattern correlates well with the distribution of DTX-binding site and both Kv1.1 and Kv1.2 mRNAs are known to be localized in cells tentatively identified as interneurones in the st. O–A (Tsaur, Sheng, Lowenstein, Jan & Jan, 1992). It is unlikely, however, that these subunits comprise the channels underlying I_K observed in the present experiments since DTX at concentrations up to 500 nM was without effect on any current component. Likewise, despite the strong expression of mRNAs of two members of the *Shaw* subfamily, Kv3.1 and Kv3.2 (Weiser *et al.* 1994) and their proteins (J. Du & C. J. McBain, unpublished observation) in interneurones of the st. O–A, it is unlikely that channels formed by these mRNAs underlie the predominant sustained current observed. Channels formed by homomeric (or heteromeric) expression of these subunits are blocked by low (<1 mM) concentrations of TEA and 4-AP. In the present experiments the IC_{50} of TEA block of the sustained current was ~7 mM and it was relatively insensitive to 4-AP. Low concentrations of 4-AP, however, removed ~10% of the sustained outward current when recorded in isolation of the transient current. Thus, channels formed by members of the *Shaw* subfamily may contribute a small component of the sustained outward current. In addition homomeric channels formed by Kv3.1b show fast deactivation kinetics ($t = 1{\cdot}5$ ms at −60 mV); it is possible that such channels formed by these subunits are responsible for the fast component of deinactivation seen in tail currents in the present experiments.

Kv2.1 mRNA is widely expressed in pyramidal neurones of the hippocampus (Kues & Wunder, 1992) and hippocampal interneurones (J. Du & C. J. McBain, unpublished observation). Homomeric channels formed by Kv2·1 activate at quite positive potentials and are blocked by TEA and 4-AP with IC_{50} values of ~10 mM and 500 μM, respectively (Frech, VanDongen, Schuster, Brown & Joho, 1989). While the sustained current observed in the present experiment shares some of the characteristics of homomeric channels formed by Kv2.1 (high threshold of activation and TEA IC_{50} of ~10 mM), these currents were not blocked by 4-AP in concentrations of up to 10 mM. Therefore at present it is impossible to clearly identify the molecular identities of the channels responsible for the sustained currents in st. O–A interneurones and further experiments using more selective antagonists are required.

In conclusion, we have shown that inhibitory cells of the st. oriens–alveus possess both transient and sustained outward potassium currents. Of the two current phenotypes it would appear that the properties of only the sustained components of the outward current are distinct from their pyramidal neurone counterparts. The transient current, in contrast, shares many of the current properties of those transient currents reported not only to exist in the pyramidal neurones but also in many neurones of the central nervous system. In the next paper we determine the role of this complement of outward currents in shaping the action potential properties as well as their role in determining the firing patterns of these cells.

Blanton, M. G., LoTurco, J. J. L. & Kriegstein, A. R. (1989). Whole cell recording from neurons in slices of reptilian and mammalian cerebral cortex. *Journal of Neuroscience Methods* **30**, 203–210.

Candia, S., Garcia, M. L. & Latorre, R. (1992). Mode of action of iberiotoxin, a potent blocker of the large conductance Ca^{2+}-activated K^+ channel. *Biophysical Journal* **63**, 583–590.

Connor, J. A. & Stevens, C. F. (1971). Voltage clamp studies of a transient outward membrane current in gastropod neural somata. *Journal of Physiology* **213**, 21–30.

Edwards, F. A., Konnerth, A., Sakmann, B. & Takahashi, T. (1989). A thin slice preparation for patch clamp recordings from synaptically connected neurones of the mammalian central nervous system. *Pflügers Archiv* **414**, 600–612.

Ficker, E. & Heinemann, U. (1992). Slow and fast transient potassium currents in cultured rat hippocampal cells. *Journal of Physiology* **445**, 431–455.

Frech, G. C., VanDongen, A. M. J., Schuster, G., Brown, A. M. & Joho, R. H. (1989). A novel potassium channel with delayed rectifier properties isolated from rat brain by expression cloning. *Nature* **340**, 643–645.

Grissmer, S., Nguyen, A. N., Aiyar, J., Hanson, D. C., Mather, R. J., Gutman, G. A., Karmilowicz, M. J., Auperin, D. D. & Chandy, K. G. (1994). Pharmacological characterization of five cloned voltage-gated K^+ channels, types Kv1.1, 1.2, 1.3, 1.5, and 3.1, stably expressed in mammalian cell lines. *Molecular Pharmacology* **45**, 1227–1234.

Gustafsson, B., Galvan, M., Grafe, P. & Wigström, H. (1982). A transient outward current in mammalian central neurones blocked by 4-aminopyridine. *Nature* **299**, 252–254.

Halliwell, J. V. (1990). *K^+ Channels in the Central Nervous System.* Halsted Press, Ellis Horwood Ltd, Chichester, UK.

Halliwell, J. V., Othman, I. B., Pelchen-Mathews, A. & Dolly, J. O. (1986). Central actions of dendrotoxin: selective reduction of a transient conductance in hippocampus and binding to localized acceptors. *Proceedings of the National Academy of Sciences of the USA* **83**, 493–497.

Hamill, O. P., Marty, A., Neher, E., Sakmann, B. & Sigworth, F. J. (1981). Improved patch-clamp techniques for high-resolution current recording from cells and cell-free membrane patches. *Pflügers Archiv* **391**, 85–100.

Kues, W. A. & Wunder, F. (1992) Heterogeneous expression patterns of mammalian potassium channel genes in developing and adult rat brain. *Journal of Neuroscience* **4**, 1296–1308.

Lacaille, J.-C., Mueller, A. L., Kunkel, D. D. & Schwartzkroin, P. A. (1987). Local circuit interactions between oriens/alveus interneurons and CA1 pyramidal cells in hippocampal slices: electrophysiology and morphology. *Journal of Neuroscience* **7**, 1979–1993.

McBain, C. J. (1994). Hippocampal inhibitory neuron activity in the elevated potassium model of epilepsy. *Journal of Neurophysiology* **72**, 2853–2863.

McBain, C. J., DiChiara, T. J. & Kauer, J. A. (1994). Activation of metabotropic glutamate receptors differentially affects two classes of hippocampal interneurons and potentiates excitatory synaptic transmission. *Journal of Neuroscience* **14**, 4433–4445.

McBain, C. J. & Dingledine, R. (1992). Dual-component miniature excitatory synaptic currents in rat hippocampal CA3 pyramidal neurons. *Journal of Neurophysiology* **68**, 17–27.

Numann, R. E., Wadman, W. J. & Wong, R. K. S. (1987). Outward currents of single hippocampal cells obtained from the adult guinea-pig. *Journal of Physiology* **393**, 331–353.

Pongs, O. (1992) Molecular biology of voltage-dependent potassium channels. *Physiological Reviews* **72**, S69–88.

Rettig, J., Wunder, F., Stocker, M., Lichtinghagen, R., Mastiaux, F., Beckh, S., Kues, W., Pedarzani, P., Schröter, K. H, Ruppersberg, J. P., Veh, R. & Pongs, O. (1992). Characterization of a Shaw-related potassium channel family in rat brain. *EMBO Journal* **11**, 2473–2486.

Rogawski, M. (1986). Single voltage-dependent potassium channels in cultured rat hippocampal neurons. *Journal of Neurophysiology* **56**, 481–493.

Ruppersberg, J. P., Ermler, M., Knopf, M., Kues, W., Jonas, P. & Koenen, M. (1993). Properties of *Shaker*-homologous potassium channels expressed in the mammalian brain. *Cellular Physiology and Biochemistry* **3**, 250–269.

Ruppersberg, J. P., Stocker, M., Pongs, O., Heinemann, S. H., Frank, R. & Koenen, M. (1991). Regulation of fast inactivation of cloned mammalian $I_{K(A)}$ channels by cysteine oxidation. *Nature* **352**, 711–714.

Sah, P., Gibb, A. J. & Gage, P. W. (1988). Potassium current activated by depolarization of dissociated neurons from adult guinea-pig hippocampus. *Journal of General Physiology* **92**, 263–278.

Serodio, P., Kentros, C. & Rudy, B. (1994). Identification of molecular components of A-type channels activating at subthreshold potentials. *Journal of Neurophysiology* **72**, 1516–1529.

Stuhmer, W., Ruppersberg, J. P., Schröter, K. H., Sakmann, B., Stocker, M., Giese, K. P., Perschke, A., Baumann, A. & Pongs, O. (1989). Molecular basis of functional diversity of voltage-gated potassium channels in mammalian brain. *EMBO Journal* **8**, 3235–3244.

Talukder, G. & Harrison, N. L. (1995). On the mechanism of modulation of transient outward current in cultured rat hippocampal neurons by di- and trivalent cations. *Journal of Neurophysiology* **73**, 73–79.

Thompson, S. H. (1977). Three pharmacologically distinct potassium channels in molluscan neurones. *Journal of Physiology* **265**, 465–488.

Thurbon, D., Field, A. & Redman, S. (1994). Electrotonic profiles of interneurons in stratum pyramidale of the CA1 region of rat hippocampus. *Journal of Neurophysiology* **71**, 1948–1958.

Traub, R. D. & Miles, R. (1991). *Neuronal Networks of the Hippocampus.* Cambridge University Press, Cambridge, UK.

Tsaur, M. L., Sheng, M., Lowenstein, D. H., Jan, Y. N. & Jan, L. Y. (1992). Differential expression of K channel mRNAs in rat brain and downregulation in the hippocampus following seizures. *Neuron* **8**, 1055–1067.

Vega-Saenz de Miera, E., Moreno, H., Fruhling, D., Kentros, C. & Rudy, B. (1992). Cloning of ShIII (Shaw-like) cDNAs encoding a novel high-voltage activating, TEA-sensitive, type-A K channel. *Proceedings of the Royal Society* B **248**, 9–18.

Weiser, M., Vega-Saenz de Miera, E., Kentros, C., Moreno, H., Franzen, L., Hillman, D., Baker, H. & Rudy, B. (1994). Differential expression of Shaw-related K^+ channels in the rat central nervous system. *Journal of Neuroscience* **14**, 949–972.

Zbicz, K. L. & Weight, F. F. (1985). Transient voltage and calcium-dependent outward currents in hippocampal CA3 pyramidal neurons. *Journal of Neurophysiology* **53**, 1038–1058.

Zhang, L. & McBain, C. J. (1995). Potassium conductances underlying repolarization and after-hyperpolarization in rat CA1 hippocampal interneurones. *Journal of Physiology* **488**, 661–672.

Received 8 December 1994; accepted 2 May 1995.